Spectral Dependence of Scattered Light in Step-Index Polymer Optical Fibers by Side-Illumination Technique

Iñaki Bikandi, María Asunción Illarramendi, Gaizka Durana, Gotzon Aldabaldetreku, and Joseba Zubia

***Abstract*—In this study, we investigate the spectral distribution of the light scattered in step-index polymer optical fibers by illuminating the fibers transversely to their symmetry axis. For that purpose, we have performed wavelength-dependent scattering measurements over the spectral range 400–750 nm in three different commercial step-index polymer optical fibers. We have estimated the mean size of the most influential scattering centers in these polymer optical fibers, analyzing theoretically the experimental results obtained.**

***Index Terms*—Polymer optical fiber (POF), scattering, side-illumination.**

I. Introduction

In the last few years, polymer optical fibers (POFs) have been widely used both for short-haul communications links, where distances to cover are generally less than one kilometer [1], and for a whole range of different sensing applications [2]. This is mainly due to their robustness, large core diameters, and high numerical apertures (NAs), which facilitate handling and light coupling [3], [4]. Among several issues, the scattering caused by the presence of inhomogeneities in the polymer affects the performance of POFs [5]. As a consequence, it limits the maximum attainable distance and the information transmission capacity of an optical link, or it compromises their sensitivity in sensing applications as well as decreases the efficiency of the optical devices. This effect, together with the absorption loss is in large part responsible for the optical energy loss and the mode coupling in POFs. For these reasons, light scattering has been extensively investigated since the early days of POFs, with studies like those carried out by Kaino *et al*. [6], [7], Koike *et al*. [5], [8] or, more recently by Bunge *et al*. [9], Aldabaldetreku *et al.* [10] and Illarramendi *et al*. [11].

Manuscript received July 3, 2014; revised August 27, 2014; accepted September 20, 2014. Date of publication September 30, 2014; date of current version October 17, 2014. This work was supported by the institutions Ministerio de Ciencia e Innovación, Gobierno Vasco/Eusko Jaurlaritza, and University of the Basque Country (UPV/EHU), under Projects TEC2012–37983- C03–01, S-PE13UN151, S-PE13CA004, IT-664-13, and UFI11/16 respectively.

I. Bikandi, G. Durana, G. Aldabaldetreku, and J. Zubia are with the Department of Communications Engineering, E.T.S.I. of Bilbao, University of the Basque Country (UPV/EHU), Bilbao 48013, Spain (e-mail: inaki.bikandi@ehu.es; gaizka.durana@ehu.es; gotzon.aldabaldetreku@ehu.es; joseba.zubia@ehu.es).

M. A. Illarramendi is with the Department of Applied Physics I, E.T.S.I. of Bilbao, University of the Basque Country (UPV/EHU), Bilbao 48013, Spain (e-mail: ma.illarramendi@ehu.es).

Color versions of one or more of the figures in this paper are available online at http://ieeexplore.ieee.org.

Digital Object Identifier 10.1109/JLT.2014.2360854

Scattering losses include Rayleigh scattering resulting from density fluctuations and compositional inhomogeneities of size much smaller than the wavelength of the propagating beam. In the Rayleigh approximation the scattering cross section is given by the expression [12]:

$$\sigma_{\text{Rayleigh}} = \frac{8\pi}{3}\left(\frac{2\pi n_{sr}}{\lambda}\right)^4\left(\frac{\phi}{2}\right)^6\left(\frac{m^2-1}{m^2+2}\right)^2 \quad (1)$$

where λ is the vacuum wavelength, ϕ is the scattering particle diameter, and m is the ratio of the refractive index of the particle (n_{scatt}) to that of the surrounding medium (n_{sr}), i.e., $m = n_{\text{scatt}}/n_{sr}$. The spectral dependence of this scattering varies inversely with the fourth power of λ. On the other hand, the scattering losses caused by nonuniformity of the fiber structure, roughness in the core-cladding interface, bubbles, cracks or other impurity particles in the fiber with sizes of the order of the wavelength, give rise to Mie scattering [12], [13]. The wavelength dependence of this type of scattering varies with the size of the inhomogeneity and with its refractive index relative to the surrounding material.

In previous works, it has been demonstrated that the side-illumination technique allows to investigate the scattered light that is able to propagate through the fiber [9]–[11]. In particular, the size of the scattering centers and their position in the fiber can be estimated from the analysis of the scattered light features with different launching conditions, either by rotating angularly the direction of the incident laser beam or by changing laterally the point of incidence on the fiber. In a previous work, we concluded that the main source of the scattering produced in some commercial step-index (SI) POFs was a scatterer, formed by fiber cladding material surrounded by fiber core material, with mean sizes ranging from 200 up to 850 nm, and placed at the core-cladding interface of the fiber [11]. Furthermore, the analysis of far-field patterns of the scattered light shown in [10] supported that the scattering center was placed at the core-cladding interface. From this experience, we propose in this work an alternative and easier method to estimate the size of the most influential scattering centers in SI POFs. Particularly, we analyze the spectral dependence of the light scattered from fiber inhomogeneities by using the side-illumination technique with a spectrally broad light source. We show that the comparison between the spectral distributions of the scattered light measured in the visible range (400–750 nm) and the corresponding theoretical curves obtained from the Mie theory can be used to estimate the size of the most important scatterers in the SI POFs. The analysis of the spectral behavior of the scattered light

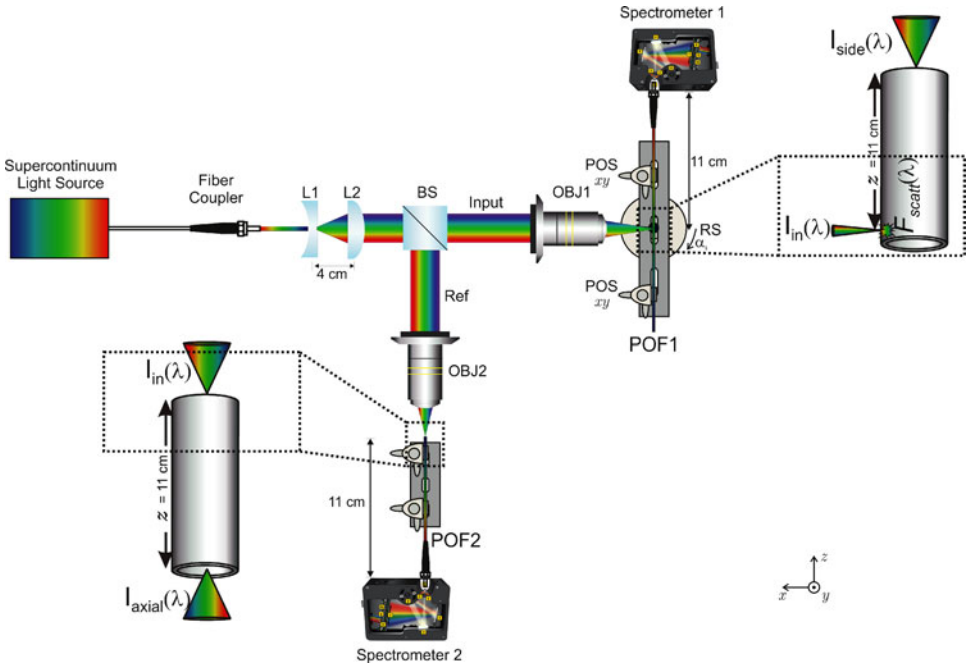

Fig. 1. Schematic diagram of the experimental setup. Legend: L1: plano-concave lens ($f' = -40$ mm); L2: plano-convex lens ($f' = +80$ mm); BS: beam splitter; OBJ1: NA 0.1 objective; OBJ2: NA 0.65 objective; POS *xy*: *xy*—micropositioner; RS: rotation stage.

TABLE I
SPECIFICATIONS OF THE MEASURED SI POFS

	SK-40	MH-4001	GH-4001
Core refractive index	1.49	1.49	1.49
Numerical Aperture	0.5	0.3	0.5
Core Diameter [μm]	980 ± 60	980 ± 60	980 ± 60
Cladding Diameter [μm]	1000 ± 60	1000 ± 60	1000 ± 60
Transmission Loss [dB/km] (650 nm)	150	160	170

is not only useful to characterize optically the fiber but it can be used for practical applications. For instance, distributed strain sensors based on POF have been designed from the analysis of the spectral behavior of scattered light in POFs [14].

II. EXPERIMENTAL

We have measured scattered light in three commercial polymethylmethacrylate (PMMA) core SI POFs from the same manufacturer (Mitsubishi) [15]: the Super ESKA SK-40 POF (named as SK-40), the MH-4001 POF (named as MH-4001), and the GH-4001-P POF (named as GH-4001). The most important properties of these SI POFs are listed in Table I.

Fig. 1 shows the experimental setup employed to measure the scattered light in the investigated POFs using the side-illumination technique. A supercontinuum and unpolarized light source, is expanded and collimated using the divergent lens (L1) and the convergent lens (L2). A reference signal (Ref) is obtained by means of a beam splitter (BS) to normalize the measurements. In order to keep both the divergence of the input beam (Input) and the spot size as small as possible, a low-numerical-aperture ($NA = 0.1$) objective (OBJ1) focuses the incident beam on the fiber side. The fiber sample is held by two *xy*-micropositioners standing on a rotation stage (RS). The RS, driven by a motion controller, allows us to change the angle of incidence α_i (also named as launching angle) along the *xz*-plane, so that we can vary the angle of incidence with respect to the perpendicular to the fiber axis. We consider positive angles when the RS moves clockwise, so that incident beam approaches to the fiber axis towards the fiber end attached to the Spectrometer. The light measured at the Spectrometer 1, $I_{\rm side}$ (λ), is the scattered light that propagates within the fiber POF1 due to the existence of inhomogeneities that deviate the direction of the incident light beam. The light measured at the Spectrometer 2, $I_{\rm axial}$ (λ), is the light transmitted along the reference fiber sample, POF2, exactly the same as POF1, when the light is focused axially on the fiber core. The propagation distance in both measurements, $I_{\rm side}$ (λ) and $I_{\rm axial}$ (λ), is the same, $z = 11$ cm. The normalization of the curve $I_{\rm side}$ (λ) by the curve $I_{\rm axial}$ (λ) cancels the spectral contribution of the absorption and scattering processes that take place along the propagation distance through the fiber. Due to the strong dependence of the propagated intensity ($I_{\rm axial}$ (λ)) on the launching conditions in short fiber samples, we have repeated the measurements of $F_{\rm scatt}$ (λ) varying the NA of objective 2 (see Fig. 1). This way, we can obtain a more precise cancellation of the light propagation effect in the measurements. Specifically, we have measured $I_{\rm axial}$ (λ) using three objective lenses, with NA values 0.65, 0.4 and 0.25. From these measurements, we have obtained a normalized mean value of $F_{\rm scatt}$ (λ), used to normalize the data, for each of the fibers analyzed. Assuming that the main source of the scattered light detected in the end of the fiber sample is placed at the core-cladding interface of the fiber [10], [11], we

define a scattering factor F_{scatt} (λ):

$$F_{\text{scatt}}(\lambda) = \frac{I_{\text{side}}(\lambda)}{I_{\text{axial}}(\lambda)} \tag{2}$$

which would describe the wavelength dependence of the intensity scattered by the scattering center placed at the core-cladding interface. The measurement of the spectral intensity from the output end of both fibers is performed by means of two AvaSpec-2048 Fiber Optic Spectrometers, with an optical resolution of 8 nm of full width at half maximum.

III. Results and Discussion

Fig. 2 shows the scattering factor F_{scatt} (λ) measured in the spectral range 400–750 nm for the three fiber samples at two launching angles: $\alpha_i = 0°$ and $\alpha_i = +45°$. In all cases, each measurement has been repeated six times and the values plotted are the mean values of the measurements, together with the standard deviations. All values are normalized to 1 at $\lambda = 400$ nm. As can be seen in the figure, the experimentally measured scattering factor decreases as the wavelength increases in all fibers analyzed. The slight ripple structure of the curves can be due to the absorption effect which may have not been perfectly cancelled in the normalization process performed in the measurements. On the other hand, we see that the spectral dependence of the experimental curves of F_{scatt} (λ) is qualitatively very similar with the incident angle α_i. In all fibers analized, the absolute value of the slope of F_{scatt} (λ) slightly decreases as the angle of incidence approaches the propagation axis of the fiber in the forward direction, that is, at $\alpha_i = +45°$. As a first approach, two theoretical curves have been included in Fig. 2, one corresponding to Rayleigh scattering (F_{scatt} (λ) ∼ 1/λ^4), and the other one corresponding to a dependence F_{scatt} (λ) ∼ 1/λ^2. This approximate spectral dependence is used by some authors to describe the scattering caused by defects of size comparable to the wavelength of the propagating beam [16]–[18]. It can be observed that the wavelength dependence of the experimental curves of F_{scatt} (λ) is closer to the spectral dependence of the type 1/λ^2 than to the Rayleigh scattering one. This fact suggests the existence of inhomogeneities of size comparable to the light wavelength. It can be noted also that the slope of the measured curves F_{scatt} (λ) for the SK-40 POF is slightly higher than that corresponding to the other two fiber samples, suggesting that the size of the inhomogeneities is smaller in this POF.

In order to gain insight into the characteristics of the main sources of the scattered light in our SI POFs, we have made use of the theoretical model developed in [11] based in the Mie theory for spheres in the independent-scatterer approximation. In this theory, it is assumed that scattering is caused by spheres placed at the core-cladding interface or in the core fiber. The scattered intensity propagating along the fiber within the critical angle is given by means of the Mie phase functions S_1 and S_2 [12]. Applying this theory for the case of a scattering sphere placed at the core-cladding interface, and formed by fiber cladding material surrounded by fiber core material, we have obtained the dependence on the wavelength and on the incident angle of the scattered intensity when light is focused on the fiber

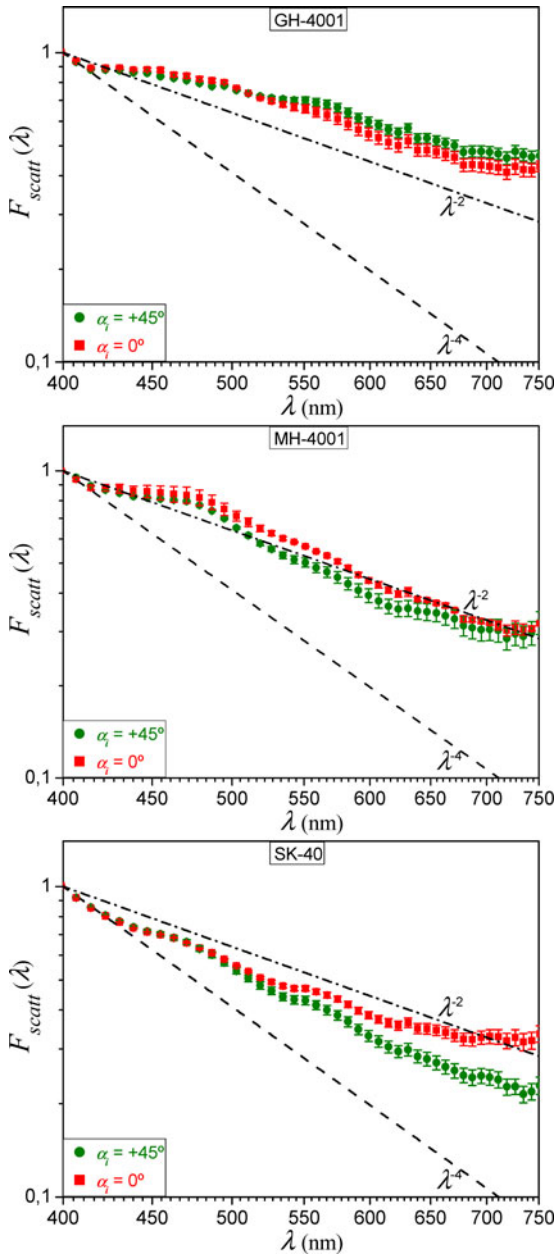

Fig. 2. Log-log plot of the scattering factor F_{scatt} (λ) for the three measured POF samples at two launching angles, ($\alpha i = 0°$ and $\alpha i = +45°$). The dashed line represents a dependence of the type 1/λ4. The dashed-dotted line represents a dependence of the type 1/λ^2.

with the incident plane along the fiber axis (*xz*-plane, see Fig. 1). This dependence, that gives the spectral dependence of F_{scatt} (λ), can be obtained from the following expression:

$$F_{\text{scatt}}(\lambda, \alpha_i) = T(\alpha_i) \int \frac{\lambda^2}{4\pi n_{\text{core}}^2} \begin{bmatrix} |S_1(\theta_{\text{IS}})|^2 \sin^2(\phi_{\text{PS}}) + \\ |S_2(\theta_{\text{IS}})|^2 \cos^2(\phi_{\text{PS}}) \end{bmatrix} d\Omega. \tag{3}$$

The calculation of F_{scatt} *(λ)* has been obtained from the intensity of the scattered light generated by scatterers placed in the core-cladding interface, $I_{TE,TM}$ (Eq. (6)) in [11, (Eq. (6))]. *TE* and *TM* denote the polarization of the incident wave: vertical

to the incident plane (*TE*) and parallel (*TM*). The scattering factor F_{scatt} *(λ)* in Eq. (3) has been calculated by averaging the scattered intensities corresponding to both polarizations. It must be noted that in this model the propagation losses of the scattered light have been neglected on the basis of the short lengths involved. The input parameters required to calculate the Mie phase functions are the wavelength of the incident wave (λ), the diameter of the scattering sphere (ϕ), and its refractive index contrast (m). In the calculations, we have taken into account the dependence on λ of the refraction index of the PMMA in the studied spectral range. θ_{IS} is the angle between the scattered beam and the incident beam on the scatterer and ϕ_{PS} is the angle between the electric field of the incident light on the scatterer and the scattering plane, (the plane formed by the incident and scattered beam). $d\Omega = \sin\theta_z d\theta_z d\phi_x$ is the element of solid angle and the integral in Eq. (3) is taken over the directions of the scattered light giving real-valued critical angle $(\theta_z)_c$. For this case it is given by [11]:

$$\sin(\theta_z)_c(\phi_x) = \frac{\sqrt{1 - n_{\mathrm{ratio}}^2}}{\cos\phi_x} \tag{4}$$

where ϕ_x is the angle of the scattered beam relative to the *x*-axis in the *xy*-plane and θ_z is the angle relative to the fiber axis (*z*-axis). n_{ratio} represents the quotient $n_{\mathrm{clad}}/n_{\mathrm{core}}$, where n_{core} and n_{clad} are, respectively, the refractive indexes of the fiber core and the fiber cladding. The expressions for θ_{IS} and ϕ_{PS} as a function of θ_z and ϕ_x are shown in [11]. The calculation of the integral of Eq. (3) has been performed for unpolarized incident light, and ϕ_x is only allowed to vary in the following ranges [11]: $0 \le \phi_x \le \arcsin(n), \pi - \arcsin(n) \le \phi_x \le \arcsin(n) + \pi$, and $2\pi - \arcsin(n) \le \phi_x \le 2\pi$. $T(\alpha_i)$ denotes the Fresnel's coefficient as a function of the incident angle (α_i) for unpolarized light.

We show in Fig. 3 the theoretical results for the factor F_{scatt} (λ) corresponding to scattering centers of different mean sizes, specifically, diameters (ϕ) from 10 to 400 nm, obtained at both launching angles ($\alpha_i = 45°$ and $\alpha_i = 0°$), together with the experimental results. The calculations have been performed using Eq. (3) and Eq. (4) with scattering centers made of cladding material ($n_{\mathrm{scatt}} = 1.42$) surrounded by core material (PMMA) placed at the core-cladding interface of the fiber. As expected, a clear dependence of the spectral distribution of the F_{scatt} (λ) curves on the scatterer size can be observed. In addition, it can be noticed that the spectral dependence theoretically calculated for a same scatterer size changes noticeably as the incident angle is varied from $\alpha_i = 0°$ to $\alpha_i = 45°$. For scatterers with small size compared to the wavelength, the calculated F_{scatt} (λ) curves show an approximated Rayleigh spectral dependence. In particular, for a mean size of 10 nm, the obtained spectral dependence shows an exact Rayleigh dependence ($1/\lambda^4$) at both incident angles. The spectral dependence of the theoretical F_{scatt} (λ) curves varies approximately as $1/\lambda^2$ for scatterers sizes around 200 nm at $\alpha_i = 0°$ and for sizes around 300 nm at $\alpha_i = 45°$.

We can conclude that the measured F_{scatt} (λ) for the three measured POF samples at both α_i are in good agreement with the theoretical F_{scatt} (λ) values corresponding to scattering centers with diameters (ϕ) within the range that goes from 200 to 400 nm. This result agrees with that obtained by means of the analysis of the variation of the scattered intensity with the incident angle [11], where a cladding scatterer with mean size of 300 ± 50 nm was estimated. The F_{scatt} (λ) curve corresponding to the SK-40 POFs presents the highest absolute value of the slope, indicating that the scattering centers are slightly smaller than those of the other fibers. If we consider the specification sheets of the three measured fibers, the results are consistent with the technical data given by the manufacturers. Specifically, with regard to the optical properties, transmission losses for the SK-40 fibers are slightly lower (<150 dB/km @ 650 nm) than for the MH-4001 and the GH-4001 fibers (<160 dB/km and <170 dB/km @ 650 nm respectively). Moreover, the SK-40 fiber is classified as the "higher grade" fiber in the Mitsubishi POF list, while the MH-4001 and GH-4001 are classified as "high reliable".

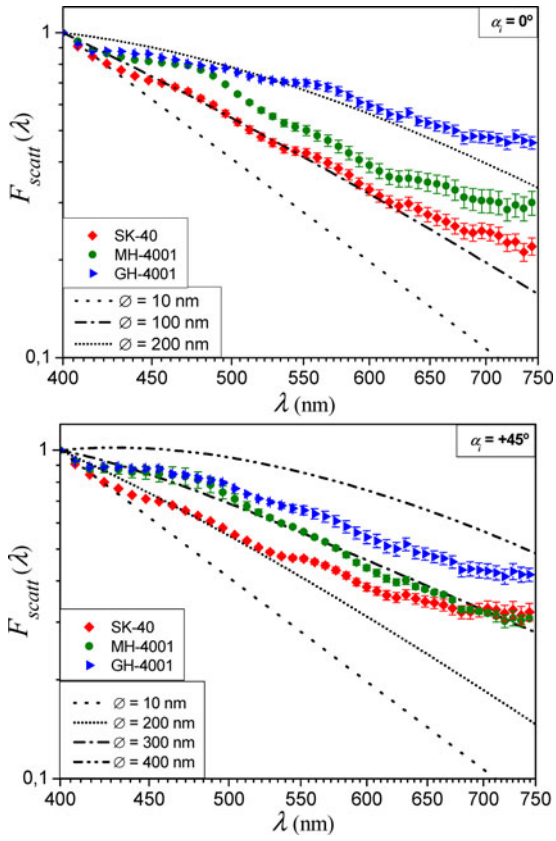

Fig. 3. Comparison of the scattering factor F_{scatt} (λ) measured for the three analyzed POF samples, with $\alpha i = 0°$ and $\alpha i = 45°$, and the theoretical values obtained for cladding scatterers surrounded by core material placed at the core-cladding interface ($m = n_{\mathrm{clad}}/n_{\mathrm{core}}$) with sizes 10 nm ≤ ϕ ≤ 400 nm.

IV. Conclusion

The spectral distribution of the scattered light in SI POFs has been investigated by using the side-illumination technique. A scattering factor F_{scatt} (λ) that describes the wavelength dependence of the scattered light originated by inhomogeneities placed at the core-cladding interface of the fiber has been defined. We have measured the spectral dependence of this scattering factor in three commercial SI POFs by exciting the samples

with a supercontinuum light source. A theoretical model based on Mie theory has been developed to simulate the obtained spectral curves. The application of this theory to experimental measurements has been used to estimate the size of the scatterers in the fibers. In agreement with previous analysis of the scattering in SI POFs, the estimated mean size of most influential sources responsible for the scattered light keeps in the range that goes from 200 to 400 nm. We have demonstrated that the spectral analysis of the scattered light in SI POF fibers by exciting them transversally to their symmetry axis provides a simple and straight-forward method for estimating the size of inhomogeneties in fibers.

REFERENCES

[1] O. Ziemann, J. Krauser, P. E. Zamzow, and W. Daum, *POF Handbook: Optical Short Range Transmission Systems*, 2nd Ed. Berlin, Germany: Springer, 2008.

[2] K. Peters, "Polymer optical fiber sensors – a review," *Smart Mater. Struct.*, vol. 20, pp. 013002–013018, 2011.

[3] T. Kaino, "Polymer optical fibers," in *Polymers for Lightwave and Integrated Optics*, L. A. Hornak, Ed. New York, NY, USA: Marcel Dekker, 1992, ch. 1.

[4] J. Zubia and J. Arrue, "Plastic optical fibers: An introduction to their technological processes and applications," *Opt. Fiber Technol.*, vol. 7, pp. 101–140, 2001.

[5] Y. Koike, N. Tanio, and Y. Ohtsuka, "Light scattering and heterogeneities in low-loss poly(methyl methacrylate) glasses," *Macromolecules*, vol. 22, pp. 1367–1373, 1989.

[6] T. Kaino, M. Fujiki, and S. Oikawa, "Low-loss plastic optical fibers," *Appl. Opt.*, vol. 20, no. 17, pp. 2886–2888, 1981.

[7] T. Kaino, M. Fujiki, and K. Jinguji, "Preparation of plastic optical fibers," *Rev. Elec. Com. Lab*, vol. 32, pp. 478–482, 1984.

[8] Y. Koike, S. Matsuoka, and H. E. Bair, "Origin of excess light scattering in poly(methyl methacrylate) glasses," *Macromolecules*, vol. 25, pp. 4807–4815, 1992.

[9] C. A. Bunge, R. Kruglov, and H. Poisel, "Rayleigh and Mie scattering in polymer optical fibers," *J. Lightw. Technol.*, vol. 24, pp. 3137–3146, 2006.

[10] G. Aldabaldetreku, I. Bikandi, M. A. Illarramendi, G. Durana, and J. Zubia, "A comprehensive analysis of scattering in polymer optical fibers," *Opt. Exp.*, vol. 18, pp. 24536–24555, 2010.

[11] M. A. Illarramendi, G. Aldabaldetreku, I. Bikandi, J. Zubia, G. Durana, and A. Berganza, "Scattering in step-index polymer optical fibers by side-illumination technique: Theory and application," *J. Opt. Soc. Amer. B*, vol. 29, pp. 1316–1329, 2012.

[12] H. C. Van De Hulst, *Light Scattering by Small Particles*. New York, NY, USA: Dover, 1981.

[13] A. W. Snyder and J. D. Love, *Optical Waveguide Theory*. London, U.K.: Chapman & Hall, 1983.

[14] P. Lenke and K. Krebber, "A new model to calculate the Rayleigh scattering profiles in polymer optical fibers for distributed strain sensing," presented at the SPIE 20th Int. Conf. Opt. Fibre Sensors, vol. 7503, Edinburgh, U.K., 2009.

[15] Mitsubishi Rayon Co., Ltd., Super ESKA plastic optical fiber [Online]. Available: http://www.pofeska.com/.

[16] F. T. Stone, "Separation of total-loss data into its absorption and scattering components: A more accurate model for fiber loss," *Appl. Opt.*, vol. 21, pp. 2721–2726, 1982.

[17] I. E. Buse *et al.*, "Wavelength dependence of the scattering loss in fluoride optical fibers," *Opt. Lett.*, vol. 15, no. 8, pp. 423–424, 1990.

[18] A. J. Cox *et al.*, "*An experiment to measure Mie and Rayleigh total scattering cross sections*," *Amer. J. Phys.*, vol. 70, no. 6, pp. 620–625, 2002.

Iñaki Bikandi received the M.Sc. and Ph.D. degrees in telecommunications engineering from the University of the Basque Country, Bilbao, Spain, in 2001 and 2013, respectively. He is currently an Assistant Professor with the Department of Communications Engineering, School of Engineering of Bilbao, University of the Basque Country.

María Asunción Illarramendi, biography not available at the time of publication.

Gaizka Durana received the B.Sc. degree in solid-state physics and the Ph.D. degree in engineering from the University of the Basque Country, Bilbao, Spain, in 1999 and 2008, respectively. He is currently an Assistant Professor with the Department of Communications Engineering, School of Engineering of Bilbao, University of the Basque Country. Dr. Durana received a European acknowledgement for the Ph.D. degree Doctor Europeus in 2008.

Gotzon Aldabaldetreku received the M.Sc. and Ph.D. degrees in telecommunications engineering from the University of the Basque Country, Bilbao, Spain, in 2000 and 2006, respectively. He is currently an Assistant Professor with the Department of Communications Engineering, School of Engineering of Bilbao, University of the Basque Country. He received a European acknowledgement for the Ph.D. degree.

Joseba Zubia received the M.Sc. degree in solid-state physics and the Ph.D. degree in physics from the University of the Basque Country, Bilbao, Spain, in 1988 and 1993, respectively. He is currently a Full Professor with the Department of Communications Engineering, School of Engineering of Bilbao, University of the Basque Country. Dr. Zubia received a Special Award for the Best Thesis in 1995 and the Euskoiker Prize in 2010.